

Gluon distribution at very small x from C-even quarkonia production at the LHC

Dmitri Diakonov, ^{a,b} M.G. Ryskin ^a and A.G. Shuvaev^{a,b}

^a*Petersburg Nuclear Physics Institute, Kurchatov National Research Centre
Gatchina, St. Petersburg 188300, Russia*

^b*St. Petersburg Academic University, St. Petersburg 194021, Russia*

E-mail: dmitri.diakonov@gmail.com, ryskin@thd.pnpi.spb.ru,
shuvaev@thd.pnpi.spb.ru

ABSTRACT: C-parity-even quarkonia $\eta_{b,c}$ and $\chi_{b,c}$ with spin 0 and 2 are produced via two-gluon fusion. The expected cross section of the inclusive production of the quarkonia at the LHC, times the branching ratios of convenient decays, is up to tens of nanobarn per unit rapidity in the case of charmonia and around one nanobarn for the bottomonia. Measuring the quarkonia production as function of rapidity will allow to determine the gluon distribution function in nucleons in a very broad range of the Bjorken x from $x \sim 10^{-2}$ where it is already known, down to $x \sim 10^{-6}$ where it is totally unknown. The scale of the gluon distribution found from such measurements turns out to be rather low, $Q^2 \simeq 2.5 - 3 \text{ GeV}^2$, for charmonia and rather large, $Q^2 \simeq 20 \text{ GeV}^2$, for bottomonia. We evaluate the scale by studying the next-to-leading-order production cross sections.

KEYWORDS: parton distribution functions, charmonia, bottomonia

ARXIV EPRINT: [1211.1578](https://arxiv.org/abs/1211.1578)

Contents

| | | |
|----------|---|-----------|
| 1 | Introduction | 1 |
| 2 | Elementary cross sections of the η_c and $\chi_{c0,2}$ production | 4 |
| 3 | The scale parameter for the gluon distribution | 6 |
| 4 | Extracting gluon distribution from the C-even charmonia production | 9 |
| 5 | Gluon distribution from the C-even bottomonia production | 11 |
| 6 | Conclusions | 13 |
| A | Appendix | 13 |

1 Introduction

The small- x gluon distribution function in nucleons at a relatively low momentum scale is a fundamental quantity in high energy physics, determining the bulk of the collision processes. Apart from being of practical importance for evaluating the rate of many processes at high energies and of the background for new physics, the gluon distribution in nucleons has its own fundamental value as it collects many fine and subtle features of Quantum Chromodynamics. At a relatively low momentum scale and small x one expects the transition from the hard DGLAP regime to the soft nonperturbative pomeron [1] but their interplay is not fully understood. Theoretical models predict various gluon distribution functions $g(x, Q^2)$, therefore, knowing it one can discriminate between the models. However, the experimental knowledge of this fundamental quantity is so far limited.

At present, the low- x global parton analysis is based mainly on the deep inelastic scattering HERA data where quark (and antiquark) but not gluon distributions are measured directly. The gluon parton distribution functions (PDFs) are extracted from the derivative $dF_2(x, Q^2)/d \ln Q^2$ using the DGLAP evolution equation. For this reason the accuracy in the determination of the gluon densities is not too good. Moreover, in the range of very small $x < 10^{-3}$ and at low momenta scale $Q^2 \simeq 2 - 3 \text{ GeV}^2$ the present-day gluon distributions are actually given by *ad hoc* extrapolations from the larger x data since this range has not been accessible by the previous data.

In Fig. 1 we plot the low- x extrapolations from the CT10 [2] and NNPDF [3, 4] gluon distributions. The drop of the gluon flux $xg(x, 2.5 \text{ GeV}^2)$ at very small x is counter-intuitive: on the contrary, one expects that it should be roughly a constant, which would correspond to a constant cross section for minijet production, or even rise as a small power of $1/x$, see Fig. 1, left. The unexpected behaviour of $g(x)$ may be a result of

neglecting power and absorptive corrections that are probably non-negligible at relatively low $Q^2 \sim 2.5 \text{ GeV}^2$. It should be noted that the MSTW low- x NLO gluon distribution [5] becomes even negative at this low scale, which gives the idea of the uncertainty in the present-day knowledge.

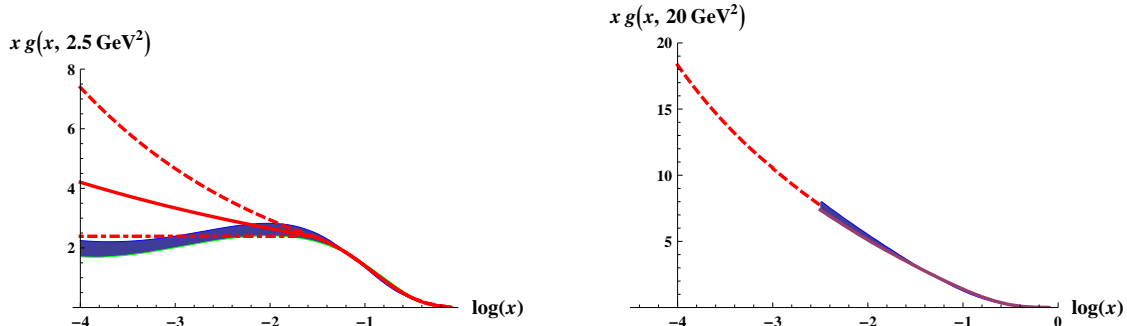


Figure 1. Gluon distribution function (times x) $xg(x, Q^2)$ for the scales $Q^2 = 2.5 \text{ GeV}^2$ appropriate for charmonia production (*left*), and $Q^2 = 20 \text{ GeV}^2$ appropriate for bottomonia production (*right*). The shadowed areas are spanning the extrapolations of the CT10 (upper side) and of the NNPDF (lower side) NLO parton distributions. The curves show our extrapolations to the small- x range assuming $xg(x) \sim \text{const.}$ (*dot-dashed lines*), $xg(x) \sim 1/x^{0.1}$ (*solid lines*) and $xg(x) \sim 1/x^{0.2}$ (*dashed lines*). On the right, the dashed line shows the extrapolation $xg(x) \sim 1/x^{0.24}$. The plots give the idea of the vast uncertainty in the present-day knowledge of the gluon distribution at very small x .

The much higher energy of the LHC and a relatively low mass of the η_c and χ_c mesons allows to probe the gluon distribution *directly* down to a few units of 10^{-6} . Indeed, the η_c with spin 0 and χ_c mesons with spin $J = 0, 2$ having positive C-parity are produced in the leading order (LO) via the simple gluon-gluon fusion $gg \rightarrow \eta_c, \chi_{c0}, \chi_{c2}$, and similarly for the bottomonia. The two-gluon fusion into spin-1 mesons such as J/Ψ and χ_{c1} is forbidden by the Landau–Yang selection rule [6], therefore the $\eta_c(0^{-+}, 2980)$, $\chi_{c0}(0^{++}, 3415)$ and $\chi_{c2}(2^{++}, 3556)$ mesons are, in this sense, privileged. A survey of quarkonia production in high energy collisions can be found in Ref. [7].

In the LO the inclusive production cross section of C-even quarkonia, integrated over the transverse momentum of a meson is given by a simple factorized equation [8]¹

$$\frac{d\sigma(pp \rightarrow \text{quarkonium})}{dY} = x_1 g(x_1, \mu_F) x_2 g(x_2, \mu_F) \hat{\sigma}(gg \rightarrow \text{quarkonium}), \quad (1.1)$$

The last factor being the fusion cross section is given in Section 2, and the values of $x_{1,2}$ are found from the kinematics as

$$x_{1,2} = \frac{M_{\text{quarkonium}}}{\sqrt{s}} e^{\pm Y} \simeq 4 \cdot 10^{-4} e^{\pm Y}. \quad (1.2)$$

It means that for the pp collision energy $\sqrt{s} = 8 \text{ TeV}$, an LHCb experiment carried out in the rapidity range $Y = 2 - 5$ is in a position to measure gluon distribution with x as small as the record $2.5 \cdot 10^{-6}$, if the lightest η_c meson is used.

¹If one does not sum over transverse momenta of the produced quarkonia there is, strictly speaking, no factorization even in the LO, and Eq. (1.1) is replaced by a more complicated expression [8].

The C-even quarkonia production is not the only way to probe low x partons. One can measure the PDFs at low x at the LHC by observing different low-mass systems, such as the Drell–Yan lepton pairs, or open heavy-quark $Q\bar{Q}$ states. The advantage of the quarkonia is their direct coupling to gluons already in the LO. In the case of charmonia with their low mass ~ 3 GeV one achieves almost the lowest possible scale where one can justify the notion of the gluon distribution itself, and the use of perturbative QCD. In fact, it is not altogether clear beforehand if the gluon distribution at a relatively low scale corresponding to the charmonia production as measured in the pp collisions is not affected by power corrections such as the absorptive effects and/or the multiple gluon rescattering, and is not different from that measured, say, in the ep collisions at the same value of Bjorken x . This important question has to be answered experimentally. The bottomonia production corresponds to a higher scale, and there is most probably no such problem there. Therefore, comparing the gluon distributions obtained from charmonia and bottomonia production one would be able to judge about the possible nonlinear effects of the gluon self-interactions at a relatively low scale.

There is also a theoretical problem with the simple LO Eq. (1.1). Supposing the inclusive b - or c -quarkonium production cross section is measured – to what precisely factorization scale μ_F does the gluon distribution correspond when extracted from Eq. (1.1)? This is an important question since one expects that the PDFs depend strongly on the choice of μ_F at low x because of the strong gluon bremsstrahlung there.

In general, after summing up all orders of the perturbation theory, the final result should not depend on the choice of μ_F that is used to separate the incoming PDFs from the hard matrix element $\hat{\sigma}$. Contributions with low virtuality, $Q^2 < \mu_F^2$, of the incoming partons are included into the PDFs, while those with $Q^2 > \mu_F^2$ are assigned to the matrix element. However, at low x the probability to emit a new gluon in an interval $\Delta\mu_F$ is enhanced by the large value of the longitudinal phase space, that is by the large value of $\ln(1/x)$. In fact, the mean number of gluons in the interval $\Delta \ln \mu_F$ is

$$\langle n \rangle \simeq \frac{\alpha_s N_c}{\pi} \ln\left(\frac{1}{x}\right) \Delta \ln \mu_F^2 \quad (1.3)$$

leading to the value of $\langle n \rangle$ up to about 8, for the case $\ln(1/x) \sim 8$ and the commonly practiced μ_F scale variation from $\mu/2$ to 2μ . Meanwhile, the next-to-leading (NLO), coefficient function (the hard matrix element), allows, by definition, the emission of only *one* additional parton. Therefore one cannot expect here a compensation between the contributions coming from the PDF and from the coefficient function. To that end one would need in this case to calculate the hard matrix element to the eighth order, which is not practical. [At large x the compensation is much better and provides reasonable stability of the predictions with respect to the variations of the scale μ_F .]

To circumvent this difficulty and to fix the factorization scale in Eq. (1.1), we use an approximate method following the recent Ref. [9]. The method is recalled in Section 3 where we also find the best choice of the factorization scale $\mu_F = \mu_0$ for the processes at hand: actually it determines at what scale parameter the gluon distributions are evaluated when the quarkonia production is measured. In the forthcoming Section 2 we evaluate the

cross sections for the elementary hard two-gluon fusion processes into C-even charmonia. It becomes possible after we go into some details of the inverse processes *i.e.* the decays of charmonia. In Section 4 we discuss the resulting inclusive production cross section of C-even charmonia, and the ways to experimentally detect them. We stress that the *absolute normalization* of the gluon distribution obtained from the measurements we suggest, can be found even in the case when the experimental and/or theoretical normalization of the cross sections is poorly known. In Section 5 we discuss briefly the production of the bottomonium χ_{b2} . The cross section is less than in the case of the charmonia production, however it can give an important independent information on the gluon distribution at a larger normalization scale. We summarize in Section 6.

2 Elementary cross sections of the η_c and $\chi_{c0,2}$ production

In the literature, one can find the LO two-gluon fusion cross sections $gg \rightarrow M$ as well as the NLO differential cross sections $gg \rightarrow M + g$ and $gq \rightarrow M + q$, expressed through the charmonia radial wave function at the origin R_0 (for the s -wave charmonium η_c) or the derivative at the origin R'_1 (for p -wave charmonia $\chi_{c0,2}$). In particular, the LO two-gluon fusion elementary cross sections are [10–12]

$$\hat{\sigma}^{\text{LO}}(gg \rightarrow \eta_c) = \frac{\pi^2 \alpha_s^2}{3} \frac{R_0^2}{M_{\eta_c}^5}, \quad (2.1)$$

$$\hat{\sigma}^{\text{LO}}(gg \rightarrow \chi_{c0}) = 12\pi^2 \alpha_s^2 \frac{R_1'^2}{M_{\chi_{c0}}^7}, \quad (2.2)$$

$$\hat{\sigma}^{\text{LO}}(gg \rightarrow \chi_{c2}) = 16\pi^2 \alpha_s^2 \frac{R_1'^2}{M_{\chi_{c2}}^7}. \quad (2.3)$$

The numerical values of the quantities R_0 and R'_1 have been evaluated in the past by many authors in the nonrelativistic quark models. Depending on the details of the model used these quantities lie in the ranges $R_0^2 \approx (0.5 - 1.0) \text{ GeV}^3$ and $R_1'^2 \approx (0.07 - 0.14) \text{ GeV}^5$. One can try to avoid model-dependent estimates and reduce the uncertainties in the couplings of two gluons to the charmonia by using the experimentally-known partial widths of the charmonia decays. We write the $C \rightarrow \gamma\gamma$ and the $C \rightarrow gg$ widths (including the 1st order QCD radiative corrections) from Ref. [13]:

$$\Gamma(\eta_c \rightarrow \gamma\gamma) = 4\pi Q_c^4 \alpha_{\text{em}}^2 \frac{f_{\eta_c}^2}{M_{\eta_c}} \left(1 + \left(\frac{20}{3} - \frac{\pi^2}{3} \right) \frac{\alpha_s}{\pi} \right), \quad (2.4)$$

$$\Gamma(\eta_c \rightarrow gg) = \frac{2}{9} 4\pi \alpha_s^2 \frac{f_{\eta_c}^2}{M_{\eta_c}} \left(1 + 4.8 \frac{\alpha_s}{\pi} \right), \quad (2.5)$$

$$\Gamma(\chi_{c0} \rightarrow \gamma\gamma) = 4\pi Q_c^4 \alpha_{\text{em}}^2 \frac{f_{\chi_{c0}}^2}{M_{\chi_{c0}}} \left(1 + \left(\frac{\pi^2}{3} - \frac{28}{9} \right) \frac{\alpha_s}{\pi} \right), \quad (2.6)$$

$$\Gamma(\chi_{c0} \rightarrow gg) = \frac{2}{9} 4\pi \alpha_s^2 \frac{f_{\chi_{c0}}^2}{M_{\chi_{c0}}} \left(1 + 8.77 \frac{\alpha_s}{\pi} \right), \quad (2.7)$$

$$\Gamma(\chi_{c2} \rightarrow \gamma\gamma) = \frac{4}{15} 4\pi Q_c^4 \alpha_{\text{em}}^2 \frac{f_{\chi_{c2}}^2}{M_{\chi_{c2}}} \left(1 - \frac{16}{3} \frac{\alpha_s}{\pi}\right), \quad (2.8)$$

$$\Gamma(\chi_{c2} \rightarrow gg) = \frac{4}{15} \frac{2}{9} 4\pi \alpha_s^2 \frac{f_{\chi_{c2}}^2}{M_{\chi_{c2}}} \left(1 - 4.827 \frac{\alpha_s}{\pi}\right), \quad (2.9)$$

where f_{η_c} , $f_{\chi_{c0}}$, $f_{\chi_{c2}}$ are the relativistic matrix elements of the local heavy-quark currents creating (or annihilating) the appropriate mesons from the vacuum. In the nonrelativistic limit they are related to the wave functions at the origin [13]:

$$f_{\eta_c}^2 = \frac{3}{\pi} \frac{R_0^2}{M_{\eta_c}}, \quad f_{\chi_{c0}}^2 = \frac{108}{\pi} \frac{R_1'^2}{M_{\chi_{c0}}^3}, \quad (2.10)$$

with $f_{\chi_{c2}} = f_{\chi_{c0}}$. The system, however, is not fully nonrelativistic, and we relax this condition.

We now fit the experimentally-known widths by Eqs. (2.4-2.9). We identify the gg widths with the total hadronic widths, $\Gamma(\eta_c \rightarrow gg) \approx \Gamma(\eta_c)_{\text{tot}}$, $\Gamma(\chi_{c0} \rightarrow gg) \approx \Gamma(\chi_{c0})_{\text{tot}} \cdot (1 - 0.0117)$, $\Gamma(\chi_{c2} \rightarrow gg) \approx \Gamma(\chi_{c0})_{\text{tot}} \cdot (1 - 0.195)$ where in the parentheses we subtract the branching ratios of the radiative decays, $Br(\chi_{c0} \rightarrow \gamma J/\psi) = 0.0117$ and $Br(\chi_{c2} \rightarrow \gamma J/\psi) = 0.195$. Here and below the experimental numbers are from the latest PDG listings [14]. We treat f_{η_c} , $f_{\chi_{c0}}$, $f_{\chi_{c2}}$ and α_s as free fitting parameters. The results of the fit are presented in Table 1, and are impressively good.

| | $\Gamma_{\text{fit}}(\gamma\gamma)$, keV | $\Gamma_{\text{exper}}(\gamma\gamma)$, keV | $\Gamma_{\text{fit}}(gg)$, MeV | $\Gamma_{\text{exper}}(\text{hadrons})$, MeV |
|----------|---|---|---------------------------------|---|
| η_c | 5.3 | 5.3 ± 0.5 | 29.7 | 29.7 ± 1.0 |
| χ_0 | 2.3 | 2.3 ± 0.23 | 10.3 | 10.3 ± 0.6 |
| χ_2 | 0.55 | 0.51 ± 0.043 | 1.48 | 1.59 ± 0.11 |

Table 1. A simultaneous fit to the radiative and to the hadronic widths of the C-even charmonia, Eqs. (2.4-2.9).

We find the best-fit values $f_{\eta_c} = 432 \text{ MeV}$, $f_{\chi_{c0}} = 240 \text{ MeV}$, $f_{\chi_{c2}} = 361 \text{ MeV}$ and $\alpha_s = 0.335$. Using these values in Eq. (2.10) and Eqs. (2.1-2.3) we obtain the elementary gluon-fusion cross sections

$$\hat{\sigma}(gg \rightarrow \eta_c) \simeq 344 \text{ nb}, \quad (2.11)$$

$$\hat{\sigma}(gg \rightarrow \chi_{c0}) \simeq 62 \text{ nb}, \quad (2.12)$$

$$\hat{\sigma}(gg \rightarrow \chi_{c2}) \simeq 140 \text{ nb}. \quad (2.13)$$

It should be kept in mind, though, that the QCD radiative corrections and the relativistic corrections to the charmonia decays appear to be rather large, therefore, the above cross sections extracted from the fit to the charmonia widths carry theoretical uncertainties. An estimate of the corrections shows that Eqs. (2.11-2.13) may be correct up to a factor of two in either direction.

Indeed, the LO cross sections of the hard gluon fusion to charmonia can be derived alternatively from simple arguments. The decay of a spin-zero meson into two on-mass-shell

gluons is described by only one helicity amplitude, call it A . In terms of this amplitude the width of a meson with mass M is $\Gamma(M \rightarrow gg) = \frac{A^2}{2\pi} M$ whereas its production cross section is $\sigma^{LO} = \frac{\pi A^2}{16M^2}$. We account here for the fact that the standard gluon PDF already includes the sum over the 8 gluon colours and over 2 transverse polarizations. A similar relation between the two-gluon fusion cross section and the two-gluon decay width exists for the spin-2 χ_{c2} meson; the only difference is the spin factor $(2J + 1)$. Therefore, the cross sections of the hard subprocesses can be written as

$$\hat{\sigma}(gg \rightarrow \eta_c) \simeq \frac{\pi^2 \Gamma(\eta_c \rightarrow gg)}{8M_{\eta_c}^3} \simeq 539 \text{ nb}, \quad (2.14)$$

$$\hat{\sigma}(gg \rightarrow \chi_{c0}) \simeq \frac{\pi^2 \Gamma(\chi_{c0} \rightarrow gg)}{8M_{\chi_{c0}}^3} \simeq 124 \text{ nb}, \quad (2.15)$$

$$\hat{\sigma}(gg \rightarrow \chi_{c2}) \simeq \frac{5\pi^2 \Gamma(\chi_{c2} \rightarrow gg)}{8M_{\chi_{c2}}^3} \simeq 85 \text{ nb}, \quad (2.16)$$

where for the numerical evaluation we have replaced the two-gluon widths by the phenomenological hadronic widths as above.

Comparing the estimates (2.11-2.13) with the estimates (2.14-2.16) one gets the idea of the theoretical uncertainty in evaluating the elementary cross sections. The first derivation takes into account the radiative corrections to the charmonia decays but ignores them in the cross sections. The second derivation is based on the fact that the effective Cgg vertex ($C = \chi_c, \eta_c$) is the same in the decay into two on-mass-shell gluons as in the fusion of two gluons (that should be considered as being on-mass-shell in the LO) into a charmonium. In both cases the radiative corrections seem to be the same. Therefore, we are inclined to trust more the second estimate (2.14-2.16), given the experience of the first one: it shows that the two-gluon decays can be well replaced by the total hadronic widths.

3 The scale parameter for the gluon distribution

To sketch the idea how to choose the appropriate scale, we start with the LO expression for the cross section. In the collinear approach, the cross section has the form

$$\sigma(\mu_F) = \text{PDF}(\mu_F) \otimes C^{\text{LO}} \otimes \text{PDF}(\mu_F), \quad (3.1)$$

where C^{LO} denotes the LO hard matrix element squared. The effect of varying the scale from m to μ_F in both PDFs can be expressed, to the first order in α_s , as

$$\sigma(\mu_F) = \text{PDF}(m) \otimes \left(C^{\text{LO}} + \frac{\alpha_s}{2\pi} \ln \left(\frac{\mu_F^2}{m^2} \right) (P_{\text{left}} C^{\text{LO}} + C^{\text{LO}} P_{\text{right}}) \right) \otimes \text{PDF}(m), \quad (3.2)$$

where the splitting functions P_{left} and P_{right} act on the left and on the right PDFs, respectively. Let us recall that in calculating the α_s correction in Eq.(3.2), the integral over the transverse momentum (virtuality) of the parton in the LO DGLAP evolution is approximated by the pure logarithmic dk^2/k^2 form. That is to say, in the collinear approach, the Leading Log Approximation (LLA) is used.

Let us now study the cross section at the NLO. First, we note that the original Feynman diagrams corresponding to the NLO matrix element C^{NLO} formally do not depend on μ_F . However, we shall see below that in fact scale dependence appears. In the NLO we can write

$$\sigma(\mu_F) = \text{PDF}(\mu_F) \otimes (C^{\text{LO}} + \alpha_s C_{\text{corr}}^{\text{NLO}}) \otimes \text{PDF}(\mu_F), \quad (3.3)$$

where we include the NLO correction to the coefficient function. In terms of Feynman diagrams it means that the $gg \rightarrow \eta_c(\chi_c)$ subprocess plus the $2 \rightarrow 2$ subprocesses, $gg \rightarrow \eta_c(\chi_c) + g$ and $qq \rightarrow \eta_c(\chi_c) + q$, are now calculated with better than the LLA accuracy. However part of this contribution is already included, to the LLA accuracy, into the second term in Eq.(3.2). Therefore this part should be now subtracted from C^{NLO} . Moreover, this LLA part depends on the scale μ_F . As a result, changing μ_F redistributes the order α_s correction between the LO part ($\text{PDF} \otimes C^{\text{LO}} \otimes \text{PDF}$) and the NLO part ($\text{PDF} \otimes \alpha_s C_{\text{rem}}^{\text{NLO}} \otimes \text{PDF}$).

We see that the part of the NLO correction that remains after the subtraction, $C_{\text{rem}}^{\text{NLO}}(\mu_F)$, depends now on the scale μ_F as due to the μ_F dependence of the LO LLA term that has been subtracted out. The trick is to choose an appropriate scale $\mu_F = \mu_0$ such as to minimize the remaining NLO contribution $C_{\text{rem}}^{\text{NLO}}(\mu_F)$. To be more precise, we choose the value $\mu_F = \mu_0$ such that as much as possible of the ‘real’ NLO contribution (which has a ladder-like form and which is strongly enhanced by the large value of $\ln(1/x)$) is included into the LO part where all the logarithmically enhanced $\alpha_s \ln(1/x)$ terms are naturally collected by the incoming parton distributions ².

As shown in Ref. [9], after the scale $\mu_F = \mu_0$ is fixed for the LO contribution the variation of the scale in the remaining NLO part does not change noticeably the predicted cross section. Moreover, it was shown that in the case of the Drell–Yan lepton pair production the NLO prediction with $\mu_F = \mu_0$ is very close to the NNLO result.

We now determine the “best” value of the scale $\mu_F = \mu_0$ for which the factorization Eq. (1.1) is maximally correct. It will be in fact the scale parameter for the gluon distribution measured from the η_c, χ_c inclusive production rates, if one uses Eq. (1.1) to determine the gluon distribution.

As explained above, in order to find the value of the appropriate scale $\mu_F = \mu_0$ of the LO contribution we have to know the cross section of hard subprocesses calculated at the NLO level. The differential cross sections of the $gg \rightarrow M + g$ and $gq \rightarrow M + q$ subprocesses as functions of the Mandelstam variables s and t are presented in Refs. [12, 17, 18] and are collected in the Appendix. We integrate them there over the available t interval, subtract the contributions generated by the last step of the LO DGLAP evolution up to the factorization scale μ_F , convoluted with the LO cross sections. Finally, we choose the value of the factorization scale $\mu_F = \mu_0$ such that it nullifies the remaining NLO $gg \rightarrow M + g$ and $gq \rightarrow M + q$ contributions.

²Actually our approach is rather close in spirit to the k_t -factorization method. Using the known NLO result we account for the exact k_t integration in the last cell adjacent to the LO hard matrix element (describing the $gg \rightarrow \eta_c(\chi_c)$ boson fusion), while the *unintegrated* parton distribution is generated by the last step of the DGLAP evolution, similarly to the prescription proposed in Refs. [15, 16].

The value of μ_0 found by this method may be in fact different for various subprocesses. It depends also on the subprocess energy \hat{s} . Therefore we have to average the $gg \rightarrow M + g$ and $gq \rightarrow M + q$ cross sections with the incoming parton flux $F(\hat{s})$ driven by the PDF low x behaviour. For low- x parton distributions, we assume a power behaviour, $F(\hat{s}) \propto \hat{s}^{-\Delta}$ with the power $0 < \Delta < 0.3$. Depending on the choice of Δ , we present in Table 2 the scale $\mu_F^2 = \mu_0^2$ that nullifies the remaining NLO contribution of the $gq \rightarrow \eta_c + q$, $gq \rightarrow \chi_c(J) + q$ and of the $gg \rightarrow \eta_c + g$, $gg \rightarrow \chi_c(J) + g$ subprocesses.

| subprocess | $\Delta = 0$ ($\hat{s} \rightarrow \infty$) | $\Delta = 0.1$ | $\Delta = 0.2$ | $\Delta = 0.3$ |
|------------------------------|---|----------------|----------------|----------------|
| $gq \rightarrow \eta_c + q$ | 3.3 | 3.1 | 2.9 | 2.75 |
| $gq \rightarrow \chi(0) + q$ | 2.4 | 2.3 | 2.2 | 2.1 |
| $gq \rightarrow \chi(2) + q$ | 2.9 | 2.8 | 2.6 | 2.5 |
| $gg \rightarrow \eta_c + g$ | 3.3 | 3.0 | 2.75 | 2.5 |
| $gg \rightarrow \chi(0) + g$ | 2.4 | 2.1 | 1.9 | 1.7 |
| $gg \rightarrow \chi(2) + g$ | 2.9 | 2.5 | 2.2 | 1.9 |

Table 2. The best scale μ_0^2 (in GeV^2) calculated from various subprocesses, depending on the power Δ in the gluon flux assumed.

In the case of an asymptotically high subenergy $\hat{s} \rightarrow \infty$, when the ladder-type diagrams dominate, the values of μ_0 are the same for both $gq \rightarrow M + q$ and $gg \rightarrow M + g$ subprocesses. However even the LHC energy is not sufficient to reach the asymptotics. Actually the rapidity interval available at the LHC, $\delta Y \simeq 10$, corresponds approximately to $\Delta \simeq 0.1$. This value looks also as realistic for the gluon distribution at low x and relatively low scale $\sim 2.5 \text{ GeV}^2$. For $\Delta > 0$ the value of μ_0 needed to nullify the remaining NLO contribution of $gq \rightarrow M + q$ subprocess is larger than that for the $gg \rightarrow M + g$ case. Let us note, however, that in the last case by changing the value of μ_F we try to mimic by the LO-generated contribution also the terms that have the structure rather different from that generated by the LO evolution. This is not altogether consistent. Therefore we believe that the value of μ_0 calculated from the $gq \rightarrow M + q$ subprocess whose Feynman diagram has the same form as that generated by the DGLAP evolution, is more reliable.

It is interesting that for the pseudoscalar η_c production we get a larger value of μ_0 despite that its mass is less than that of $\chi_{c0,2}$. Owing to the unnatural parity of η_c , the production vertex contains an additional transverse momentum that enhances large- $|t|$ contributions. To compensate it, one has to take a larger μ_0 .

We see from Table 2 that we still have some $\sim 10 - 20\%$ uncertainty in the value of the appropriate scale μ_0 but this is much less than the usually used *ad hoc* interval from $M/2$ up to $2M$. Moreover, when and if it comes to fitting the data it will be possible to simultaneously specify/determine the value of Δ and to fix the appropriate scale $\mu_F = \mu_0$ more precisely. At the moment we think that the power $\Delta = 0.1$ is the most realistic for a relatively low scale $\mu_F^2 = 2 - 3 \text{ GeV}^2$.

4 Extracting gluon distribution from the C-even charmonia production

Choosing the appropriate scale $\mu_F = \mu_0$ from Table 2 we strongly suppress the remaining higher α_s order contributions to the LO factorization Eq. (1.1). Thus, the inclusive cross section of the η_c and $\chi_{c0,2}$ production

$$\frac{d\sigma}{dY} = x_1 g(x_1, \mu_0) x_2 g(x_2, \mu_0) \hat{\sigma}(gg \rightarrow C\text{-even charmonium}) \quad (4.1)$$

will measure directly the product of gluon densities at the normalization point μ_0 . The values of $x_{1,2}$ are found from Eq. (1.2) while the values of $\hat{\sigma}$ are given by Eqs. (2.14-2.16).

For example, at $\sqrt{s} = 8$ TeV and $Y = 5$ we have for the η_c production $x_1 = 0.055$, $x_2 = 2.5 \cdot 10^{-6}$, and for the χ_{c2} production $x_1 = 0.066$, $x_2 = 3.0 \cdot 10^{-6}$. At the upper side (x_1) the gluon distribution is rather accurately established, therefore from measuring the rate of the charmonia production one can find the gluon densities at unprecedented low x_2 , see in more detail below.

Let us briefly discuss how to register the production of the η_c and χ_c mesons. Of the three C-even charmonia considered the most favourable observational conditions seem to be for the χ_{c2} meson via an anomalously large radiative decay $\text{Br}(\chi_{c2} \rightarrow \gamma J/\psi) = 0.195 \pm 0.008$. Actually the χ_{c2} inclusive production has been already observed at the LHCb via this particular decay channel [19]. The expected χ_{c2} production rate, times this branching ratio, times the branching ratio $\text{Br}(J/\psi \rightarrow \mu^+ \mu^-) = (5.93 \pm 0.06) \cdot 10^{-2}$ is plotted in Fig. 2. It appears to be quite large – in the range of tens of nanobarns.

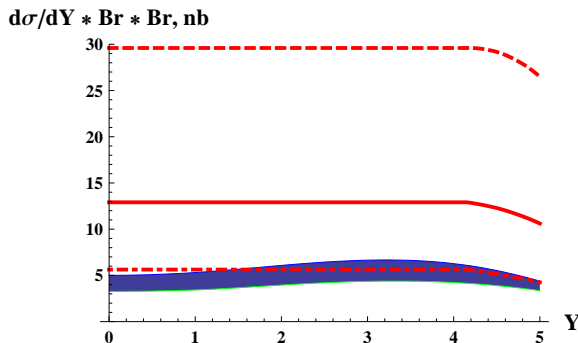


Figure 2. Cross section of the inclusive χ_{c2} production per unit rapidity Y , times the branching ratio of its decay into $\gamma J/\psi$, times the branching ratio of the $J/\psi \rightarrow \mu^+ \mu^-$ decay, in nanobarns. The shaded area corresponds to the gluon flux from the shaded area in Fig. 1, whereas the dot-dashed, solid and dashed curves correspond to the extrapolation using $x g(x) \sim \text{const.}$ ($\Delta = 0$), $x g(x) \sim 1/x^{0.1}$ ($\Delta = 0.1$), and $x g(x) \sim 1/x^{0.2}$ ($\Delta = 0.2$), respectively, shown in Fig. 1, left. The scale parameter $\mu_0^2 = 2.5 \text{ GeV}^2$ is assumed for the gluon distribution.

The χ_{c0} meson has a comparable production rate but a much smaller radiative decay branching ratio $\text{Br}(\chi_{c0} \rightarrow \gamma J/\psi) = 0.0117 \pm 0.008$. The production times branching curves for the χ_{c0} meson are similar to those shown in Fig. 2 but the overall scale is an order of magnitude less. Therefore, unless a good hadronic decay channel is found, the χ_{c0} meson cannot compete with its χ_{c2} cousin.

Finally, the η_c meson decays mainly into π, K mesons and it is not easy to find a meson decay mode that would not be plagued by the huge multi-meson combinatorial background at the LHC energies. Probably the best channel would be the decay into $p\bar{p}$ with the branching ratio $\text{Br}(\eta_c \rightarrow p\bar{p}) = (1.41 \pm 0.17) \cdot 10^{-3}$ or into $\Lambda\bar{\Lambda}$ with the branching ratio $\text{Br}(\eta_c \rightarrow \Lambda\bar{\Lambda}) = (0.94 \pm 0.32) \cdot 10^{-3}$. The η_c cross section times the $p\bar{p}$ branching is similar and close in magnitude to what is presented in Fig. 2 for the χ_{c2} meson. It should be noted that the η_c production measures, paradoxically, the gluon distribution at a larger scale than the χ_{c2} meson (see Section 3) and therefore the two measurements can be of independent value.

It is interesting that when in the whole x region probed by an experiment the gluon distribution has the power-law form $g(x) \sim 1/x^{1+\Delta}$ the production cross section is independent on the rapidity Y of the charmonia produced. However the height of the plateau is extremely sensitive to the power Δ at small x .

Remarkably, even if one does not know the absolute normalization of the experimental cross section for the charmonia production and/or of the theoretical cross section (4.1), one can still extract the *absolute normalization* of the gluon distribution at low x , by matching the measurements with the distribution in the medium- x range where it is already known.

To give the idea, let us consider the setup of the LHCb where particles with rapidity up to $Y = 5$ can be registered. Supposing it is found that the number of counts $C(Y)$ of the χ_{c2} mesons produced in a rapidity interval $Y \pm \delta Y$ is roughly independent of Y , corresponding to the plateau in Fig. 2. It means that the gluon distribution at very small x has a power-law behaviour, $x g(x) = a x^{-\Delta}$. We want to find the power Δ and the absolute normalization a . We write

$$x_1 g(x_1) x_2 g(x_2) = \mathcal{N} C(Y), \quad x_{1,2} = \frac{M_{\chi_{c2}}}{\sqrt{s}} e^{\pm Y}, \quad (4.2)$$

$$a^2 \left(\frac{M_{\chi_{c2}}^2}{s} \right)^{-\Delta} = \mathcal{N} C(Y), \quad (4.3)$$

where \mathcal{N} is an unknown normalization factor³. We see from Eq. (4.3) that the power law for $g(x)$ is the only one leading to the number of counts $C(Y)$ independent of the rapidity.

However, at $Y > 4$ the number of counts will deviate from the plateau, see Fig. 2. This is where one of the two fusing gluons has a known flux $x_1 g(x_1)$, see the solid part of the curve at the right-hand side of Fig. 3. At the end point of the solid curve, that is at $x = x_c \approx 0.028$ the gluon distribution is still known to an accuracy of a few percent⁴. Therefore, one can determine the other gluon's $x_2 g(x_2)$ from Eq. (4.2):

$$\frac{1}{\mathcal{N}} x_2 g(x_2) = \frac{C(Y)}{x_1 g(x_1)} = \frac{a}{\mathcal{N}} x_2^{-\Delta}. \quad (4.4)$$

To find numerically Δ and $\frac{a}{\mathcal{N}}$, one has to make two or more measurements at $Y > 4$, for example as shown in Fig. 3, and make a two-parameter fit to Eq. (4.4). Then, assuming

³In fact \mathcal{N}^{-1} is the elementary fusion cross section (2.13), times the integrated luminosity, times the registration efficiency.

⁴The accuracy can be estimated by comparing two known gluon distributions [2–4] at x_c .

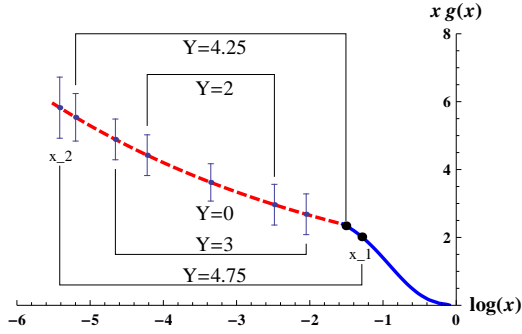


Figure 3. Finding the gluon distribution $xg(x)$ from Eq. (4.2). The solid part of the curve shows the known distribution at the normalization point $\mu_0^2 = 2.5 \text{ GeV}^2$. The dashed part is the supposed power law at very small x , $xg(x) = ax^{-\Delta}$. The rectangular “gates” indicate the values of x_1 (right point) and x_2 (left point) in the product of the gluon distributions, corresponding to a given rapidity Y of the χ_{c2} meson produced. $\sqrt{s} = 8 \text{ TeV}$ is assumed.

the power behaviour of the gluon distribution all the way up to x_c we equate

$$\frac{a}{\mathcal{N}} x_c^{-\Delta} = \frac{1}{\mathcal{N}} x_c g(x_c). \quad (4.5)$$

In this equation, the combination $\frac{a}{\mathcal{N}}$ is presumably known from the fit above, and all the rest quantities are also known, except the normalization factor \mathcal{N} . Therefore, Eq. (4.5) enables one to find \mathcal{N} and hence the absolute normalization of the gluon distribution a .

Alternatively, one can find Δ , a and \mathcal{N} separately by solving the system of equation (4.3) and two equations (4.4) evaluated at two different rapidities $Y > 4$.

If the actual behaviour of the gluon distribution at very low x is substantially different from power-like, this will be seen from the deviation from the flat plateau in the production rate as function of Y . The data should be then analyzed accordingly, however in any case the absolute normalization of the gluon distribution will be possible to deduce even without knowing the absolute values of the charmonia production cross section – by matching the data with the gluon distribution at $x \geq x_c \approx 0.028$ where it is already known with a reasonable accuracy.

We would like to remark that a good complement would be measuring charmonia production in a fixed-target experiment with the LHC beams (AFTER@LHC) as it allows to observe charmonia with low p_T and to extract the gluon distribution at x from a few units of 10^{-3} to $x \sim 1$ [20, 21]⁵.

5 Gluon distribution from the C-even bottomonia production

The same theoretical considerations can be applied to measuring gluon distributions from the production of the C-even $b\bar{b}$ mesons, such as $\chi_{b2}(1P)(2^{++}, 9912)$. Like χ_{c2} , the bottomonium χ_{b2} has a large branching ratio for the radiative decay, $\text{Br}(\chi_{b2}(1P) \rightarrow \gamma\Upsilon(1S)) = 0.191 \pm 0.012$ while the leptonic branching ratio for the Υ is $\text{Br}(\Upsilon(1S) \rightarrow \mu^+\mu^-) =$

⁵We thank J.-P. Lansberg for bringing our attention to this work.

$(2.48 \pm 0.05) \cdot 10^{-2}$. This decay cascade makes the observation of the bottomonium $\chi_{b2}(1P)$ possible.

At large heavy-quark masses, the gluon-fusion cross sections of the quarkonia production scale as $\sigma(gg \rightarrow \chi) \sim \alpha_s^2(M_\chi)/M_\chi^2$ and therefore the χ_b cross section is expected to be ~ 20 times less than that of χ_c . From the evaluation of the χ_{c2} production cross section (2.16) we estimate $\sigma(gg \rightarrow \chi_{b2}(1P)) \approx 4$ nb. The $\chi_{b2}(2P)$ production cross section must be 3 – 4 times smaller, according to the nonrelativistic estimate of $R_1'(0)$.

However, the smaller elementary χ_{b2} production cross section is multiplied in Eq. (4.1) by a larger gluon flux $x_1 g(x_1, \mu_0^2) x_2 g(x_2, \mu_0^2)$ expected at the scale μ_0^2 appropriate for the bottomonia as contrasted to the charmonia. According to the derivation in Section 3, the scale μ_0^2 is proportional to the mass squared of the quarkonium in question. It is known that at higher resolution scale the gluon distribution increases towards small x effectively as a higher power $x^{-\Delta}$. Taking $\Delta \approx 0.25$ and using Table 2 we find that for the χ_{b2} production the gluon distribution scale is $\mu_0^2 \approx 20 \text{ GeV}^2$; it is plotted in Fig. 1, right.

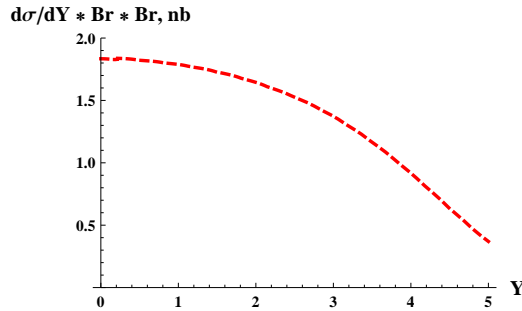


Figure 4. The expected cross section of the inclusive bottomonium $\chi_{b2}(1P)$ production per unit rapidity Y , times the branching ratio of its decay into $\gamma\Upsilon(1S)$, times the branching ratio of the $\Upsilon(1S) \rightarrow \mu^+\mu^-$ decay, in nanobarns. The gluon distribution shown in Fig. 1, right, is assumed.

The expected cross section of the inclusive bottomonium $\chi_{b2}(1P)$ production, times the branching ratio of its decay into $\gamma\Upsilon(1S)$, times the branching ratio of the $\Upsilon(1S) \rightarrow \mu^+\mu^-$ decay, is plotted in Fig. 4, right. It is not a plateau anymore, even if one assumes a power-law behaviour of the gluon distribution at low x . We see that it is a few times less than the inclusive χ_{c2} production, times its branching ratios, see Fig. 2, but probably within reach.

The bottomonium $\chi_{b2}(2P)(2^{++}, 10269)$ can be observed via the radiative decay into the two Υ 's with the branching ratios $\text{Br}(\chi_{b2}(2P) \rightarrow \gamma\Upsilon(1S)) = 0.071 \pm 0.01$ and $\text{Br}(\chi_{b2}(2P) \rightarrow \gamma\Upsilon(2S)) = 0.162 \pm 0.024$. The consequent leptonic branching ratios for the Υ decays are $\text{Br}(\Upsilon(1S) \rightarrow \mu^+\mu^-) = (2.48 \pm 0.05) \cdot 10^{-2}$ and $\text{Br}(\Upsilon(2S) \rightarrow \mu^+\mu^-) = (1.93 \pm 0.17) \cdot 10^{-2}$, respectively. Combining these decay cascades, the total registration rate of the $\chi_{b2}(2P)$ bottomonium is expected to be very similar to that shown in Fig. 4, right, being however 3 – 4 times less.

Although the production cross section (times the branching ratios) for $\chi_{b2}(1P)$ is several times less than that for $\chi_{c2}(1P)$, it would be easier to match the measured gluon distribution at very low x to that already known at larger values of x , see the end of Section 5. The smallest value of x accessible from the bottomonium production is $x_{\min} = 8.3 \cdot 10^{-6}$.

It should be noted that the χ_{b2} must have a broad distribution in the transverse momenta as due to the typical double-logarithmic QCD form factor [8].

6 Conclusions

The inclusive production cross sections of C-even charmonia $\chi_{c2}(2^{++}, 3556)$ and $\eta_c(0^{-+}, 2998)$ at the LHC, times the branching ratios of their convenient decay modes, $\text{Br}(\chi_{c2} \rightarrow \gamma J/\psi) \cdot \text{Br}(J/\psi \rightarrow \mu^+ \mu^-)$ and $\text{Br}(\eta_c \rightarrow p\bar{p})$, respectively, are estimated to lie in the range 5 – 30 nb, depending on what is the actual behaviour of the gluon distribution at very low Bjorken x . Measuring the production of those charmonia, integrated over their transverse momenta will enable one to determine the fundamental quantity — the gluon distribution in nucleons $g(x, Q^2)$ — at an unprecedented low $x \geq 2.5 \cdot 10^{-6}$ and relatively low normalization scale $Q^2 = 2.5 - 3 \text{ GeV}^2$. The absolute normalization of the gluon distribution can be found by matching the measured charmonia yield with the gluon distribution at higher x where it is already known, even if the normalization of the experimental and/or theoretical cross sections are not well established.

Similarly, measuring the inclusive production of the bottomonium $\chi_{b2}(2^{++}, 9912)$ with the cross section times the branching ratios around 1 nb will allow to extract the gluon distribution at $x \geq 8.3 \cdot 10^{-6}$ but a larger scale $Q^2 \approx 20 \text{ GeV}^2$.

Combining the measurements of the two quarkonia production will give a rather full knowledge of the fundamental quantity – the gluon distribution – in a broad range of x and Q^2 . In particular, one will be in a position to judge if at $Q^2 = 2.5 - 3 \text{ GeV}^2$ the nonlinearity (the gluon self-interaction) becomes important or not, and to discriminate between various theoretical models of the high-energy processes.

Acknowledgments

We thank Alexey A. Vorobyev and Mark Strikman for helpful discussions. This work has been supported in part by the grants RSGSS-4801.2012.2 and RFBR 11-02-00120-a. D.D. acknowledges partial support by the Japan Society for the Promotion of Sciences and thanks the RCNP at Osaka University where this work has been finalized, for hospitality.

A Appendix

We list below the LO and NLO cross sections of η_c and χ_c mesons production [12, 17, 18]. We have checked the equations and present them in the form which is further on used for integrating the differential cross sections over t .

The LO contributions to the hard $gg \rightarrow \chi_c(J=0, 2)$ and $gg \rightarrow \eta_c(J=0)$ subprocesses, *i.e.* the LO two-gluon fusion cross sections are given by Eqs. (2.1-2.3).

The NLO $2 \rightarrow 2$ differential cross sections are expressed through the quantity \hat{s} denoting the $\chi + g$, $\chi + q$ or $\eta + g$, $\eta + q$ energy squared, $r = \hat{s}/M^2$. The variable z is defined by the equation $\hat{t} = -\hat{s}(1 - 1/r + z)/2$, where \hat{t} is the momentum transfer squared from the initial to the final gluon or quark.

The NLO cross section is obtained by integrating the differential cross section over \hat{t} , that is translated in our notations into the integration over z . The divergencies of the integrands at $z = 1 - 1/r$ or at $z = -1 + 1/r$ reflect the logarithmic divergencies of the differential cross sections at $\hat{t} \rightarrow 0$ or at $\hat{u} = M^2 - \hat{s} - \hat{t} \rightarrow 0$. They are the collinear singularities that are responsible for the evolution of the PDF,

$$\left. \frac{d\hat{\sigma}^{NLO}}{dt} \right|_{t \rightarrow 0} = -\frac{1}{\hat{t}} \hat{\sigma}^{LO} K(1/r)r,$$

where $K(x)$ is LO DGLAP splitting function for the gg or the qg channels. To avoid the double counting we subtract from the NLO cross sections the logarithmic part at $z > 1 - 1/r - 2\mu_F^2/\hat{s}$ (and at $z < -1 + 1/r + 2\mu_F^2/\hat{s}$ if there is a singularity in \hat{u}) as being attributed to the PDF, thereby removing the infrared divergency at $t \rightarrow 0$.

Since the NLO $qg \rightarrow qM$ cross section is described by the same diagram as that responsible for the LO DGLAP evolution we choose the scale $\mu_F = \mu_0$ such that being integrated up to μ_0 the LO-generated contribution nullifies the remaining NLO $qg \rightarrow qM$ cross section. By doing that we shift the major part of the corrections (enhanced by the large value of $\ln(1/x)$) to the low x parton distributions. Below we list the NLO cross sections used in this derivation.

The $gg \rightarrow g + \chi_c(0)$ differential cross section is

$$\frac{d\hat{\sigma}(gg \rightarrow g + \chi_c(0))}{dt} = \frac{\pi\alpha_S^3 R_1'^2}{32\hat{s}^2 M_{\chi_c(0)}^5} F_{gg}^X(0), \quad F_{gg}^X(0) = N_{gg}^X(0)/D_{gg}^X(0) \quad (\text{A.1})$$

where

$$\begin{aligned} N_{gg}^X(0) = & -32[3(154r + 27) + (z^2 + 3)^4(z^2 - 1)^2r^{14} - 12(76z^2 + 159)r^3 \\ & - (270z^2 - 187)r^2 + 2(87z^4 + 848z^2 + 649)r^5 + (279z^4 + 1004z^2 - 663)r^4 \\ & - 2(3z^6 + 25z^4 + 85z^2 + 47)(z^2 + 3)^2(z^2 - 1)r^{13} \\ & - (36z^6 + 893z^4 + 3418z^2 - 4875)r^6 + 8(42z^6 + 517z^4 + 1268z^2 - 507)r^7 \\ & + 2(69z^6 - 531z^4 - 6217z^2 - 5193)(z^2 - 1)r^9 \\ & - (81z^8 + 1760z^6 + 5858z^4 + 16312z^2 + 7669)r^8 \\ & + (18z^{10} + 1249z^8 + 10424z^6 + 34958z^4 + 21726z^2 + 2025)r^{10} \\ & - 4(48z^{10} + 661z^8 + 3172z^6 + 7958z^4 + 5604z^2 + 1757)r^{11} \\ & + (9z^{12} + 212z^{10} + 1809z^8 + 5952z^6 + 11019z^4 + 5516z^2 + 1083)r^{12}], \end{aligned}$$

$$D_{gg}^X(0) = (rz + r + 1)^4(rz + r - 1)(rz - r + 1)(rz - r - 1)^4(r - 1)^4r.$$

We integrate it over t and obtain

$$\hat{\sigma}^{NLO}(gg \rightarrow g + \chi_c(0)) = \frac{\pi\alpha_S^3 R_1'^2}{64\hat{s}M_{\chi_c(0)}^5} T_{gg}^X(0) \quad (\text{A.2})$$

where

$$\begin{aligned}
T_{gg}^X(0) = & \left[64 \left((108 \ln \frac{\hat{s} - M_X^2}{\mu_F^2} (r^2 - r + 1)^2 (r + 1)^4 (r - 1)^2 \right. \right. \\
& - (172r^{10} - 56r^9 - 617r^8 + 188r^7 + 1104r^6 - 508r^5 + 302r^4 \\
& + 52r^3 + 92r^2 + 132r + 99) (r^2 - 1) \\
& - 12(9r^{11} - 31r^9 + 14r^8 + 40r^7 - 10r^6 - 176r^5 + 42r^4 + 7r^3 \\
& \left. \left. + 10r^2 - 41r - 24) \ln(r)r \right) \right] / [3(r + 1)^5 (r - 1)^4 r^2].
\end{aligned}$$

The $gg \rightarrow g + \chi_c(2)$ differential cross section is

$$\frac{d\hat{\sigma}(gg \rightarrow g + \chi_c(2))}{dt} = \frac{3\pi\alpha_S^3 R_1'^2}{32\hat{s}^2 M_{\chi_c(2)}^5} F_{gg}^X(2), \quad F_{gg}^X(2) = N_{gg}^X(2) / D_{gg}^X(2) \quad (\text{A.3})$$

where

$$\begin{aligned}
N_{gg}^X(2) = & 64 \left[6(28r + 9) + (z^2 + 3)^4 (z^2 - 1)^2 r^{14} \right. \\
& + 6(5z^2 - 34)r^3 - 5(36z^2 + 103)r^2 + 2(93z^4 + 1405z^2 + 2022)r^4 \\
& - 2(519z^4 + 1567z^2 + 2762)r^5 - 2(3z^6 - 32z^4 + 199z^2 - 10)(z^2 + 3)^2 (z^2 - 1)r^{13} \\
& - (24z^6 + 3017z^4 + 10102z^2 + 3705)r^6 + 4(315z^6 + 2264z^4 + 5635z^2 + 2154)r^7 \\
& - 2(27z^8 + 178z^6 + 760z^4 + 7742z^2 + 605)r^8 \\
& - 4(93z^8 + 1197z^6 + 4055z^4 - 281z^2 + 216)r^9 \\
& + (12z^{10} + 1099z^8 + 8732z^6 + 29186z^4 + 6336z^2 - 309)r^{10} \\
& - 2(21z^{10} + 482z^8 + 4190z^6 + 13432z^4 + 837z^2 + 1006)r^{11} \\
& \left. + 2(3z^{12} - 11z^{10} + 186z^8 + 2634z^6 + 5991z^4 - 2927z^2 + 780)r^{12} \right],
\end{aligned}$$

$$D_{gg}^X(2) = 3(rz + r + 1)^4 (rz + r - 1)(rz - r + 1)(rz - r - 1)^4 (r - 1)^4 r.$$

We integrate it over t and obtain

$$\hat{\sigma}^{NLO}(gg \rightarrow g + \chi_c(2)) = \frac{3\pi\alpha_S^3 R_1'^2}{64\hat{s} M_{\chi_c(2)}^5} T_{gg}^X(2) \quad (\text{A.4})$$

where

$$\begin{aligned}
T_{gg}^X(2) = & \left[128 \left((72 \ln \frac{\hat{s} - M_X^2}{\mu_F^2} (r^2 - r + 1)^2 (r + 1)^4 (r - 1)^2 \right. \right. \\
& - (106r^{10} - 32r^9 - 101r^8 + 239r^7 + 651r^6 - 793r^5 + 395r^4 \\
& - 527r^3 + 35r^2 + 201r + 66) (r^2 - 1) \\
& - 12(6r^{11} - 22r^9 + 8r^8 - 74r^7 - 31r^6 \\
& \left. \left. - 11r^5 + 204r^4 - 86r^3 - 17r^2 - 5r - 12) \ln(r)r \right) \right] / [9(r + 1)^5 (r - 1)^4 r^2].
\end{aligned}$$

The $gg \rightarrow g + \eta_c$ differential cross section is

$$\frac{d\hat{\sigma}(gg \rightarrow g + \eta)}{dt} = \frac{\pi\alpha_S^3 R_0^2}{4\hat{s}^2 M_\eta^3} F_{gg}^\eta, \quad F_{gg}^\eta = N_{gg}^\eta / D_{gg}^\eta \quad (\text{A.5})$$

where

$$N_{gg}^\eta = -(r^4 z^4 + 6r^4 z^2 + 9r^4 - 12r^3 z^2 - 4r^3 + 6r^2 z^2 + 6r^2 - 4r + 9)(r^2 z^2 + 3r^2 - 2r - 1)^2,$$

$$D_{gg}^\eta = (rz + r + 1)^2(rz + r - 1)(rz - r + 1)(rz - r - 1)^2(r - 1)^2 r.$$

We integrate it over t and obtain

$$\hat{\sigma}^{NLO}(gg \rightarrow g + \eta) = \frac{\pi \alpha_S^3 R_0^2}{8 \hat{s} M_\eta^3} T_{gg}^\eta \quad (\text{A.6})$$

where

$$T_{gg}^\eta = \left[2 \left(12 \ln \frac{\hat{s} - M_\eta^2}{\mu_F^2} (r^2 - r + 1)^2 (r + 1)^2 - (12r^6 + 23r^4 + 24r^3 + 2r^2 + 11)(r^2 - 1) - 12(r^7 - 5r^5 - 2r^4 - r^3 - 3r - 2) \ln(r)r \right) \right] / [3(r + 1)^3 (r - 1)^2 r^2].$$

The $qg \rightarrow q + \chi_c(0)$ differential cross section is

$$\frac{d\hat{\sigma}(qg \rightarrow q + \chi_c(0))}{dt} = \frac{32\pi\alpha_s R_1'^2}{9\hat{s}^2 M_{\chi_c(0)}^5} F_{qg}^\chi(0), \quad F_{qg}^\chi(0) = N_{qg}^\chi(0)/D_{qg}^\chi(0) \quad (\text{A.7})$$

where

$$N_{qg}^\chi(0) = (r^2(z^2 - 2z + 5) + 2rz - 2r + 1)(rz + r + 5)^2, \\ D_{qg}^\chi(0) = 2(rz + r + 1)^4(rz + r - 1).$$

We integrate it over t and obtain

$$\hat{\sigma}^{NLO}(qg \rightarrow g + \chi_c(0)) = \frac{16\pi\alpha_S^3 R_1'^2}{9\hat{s} M_{\chi_c(0)}^5} T_{qg}^\chi(0) \quad (\text{A.8})$$

where

$$T_{qg}^\chi(0) = \left[27 \left(\ln \frac{\hat{s} - M_\chi^2}{\mu_F^2} (2r^2 - 2r + 1)r - 2(43r^2 - 14r + 4)(r - 1) - 6(9r^2 - 9r + 4) \ln(r)r \right) \right] / (6r^2).$$

The $qg \rightarrow q + \chi_c(2)$ differential cross section is

$$\frac{d\hat{\sigma}(qg \rightarrow q + \chi_c(2))}{dt} = \frac{32\pi\alpha_s R_1'^2}{3\hat{s}^2 M_{\chi_c(2)}^5} F_{qg}^\chi(2), \quad F_{qg}^\chi(2) = N_{qg}^\chi(2)/D_{qg}^\chi(2) \quad (\text{A.9})$$

where

$$N_{qg}^\chi(2) = [r^4(z^4 + 2z^2 + 8z + 5) - r^3(44z^2 + 8z - 36) + r^2(22z^2 - 48z + 34) + 48rz - 4r + 25], \\ D_{qg}^\chi(2) = (3(rz + r + 1)^4(rz + r - 1)).$$

We integrate it over t and obtain

$$\hat{\sigma}^{NLO}(qg \rightarrow q + \chi_c(2)) = \frac{16\pi\alpha_s R_1'^2}{3\hat{s}M_{\chi_c(2)}^5} T_{qg}^\chi(2) \quad (\text{A.10})$$

where

$$T_{qg}^\chi(2) = \left[18 \ln \frac{\hat{s} - M_\chi^2}{\mu_F^2} (2r^2 - 2r + 1)r - (53r^2 - 16r + 20)(r - 1) - 3(12r^2 - 12r + 5) \ln(r)r \right] / (9r^2).$$

The $qg \rightarrow q + \eta_c$ differential cross section is

$$\frac{d\hat{\sigma}(qg \rightarrow q + \eta)}{dt} = \frac{4\pi\alpha_s R_0^2}{9\hat{s}^2 M_{\eta_c}^3} F_{qg}^\eta, \quad F_{qg}^\eta = N_{qg}^\eta / D_{qg}^\eta \quad (\text{A.11})$$

where

$$N_{qg}^\eta = 2(z - 1)r + 1 + (z^2 - 2z + 5)r^2, \\ D_{qg}^\eta = (rz + r + 1)^2(rz + r - 1).$$

We integrate it over t and obtain

$$\hat{\sigma}^{NLO}(qg \rightarrow g + \eta) = \frac{2\pi\alpha_s^3 R_0^2}{9\hat{s}M_\eta^3} T_{qg}^\eta \quad (\text{A.12})$$

where

$$T_{qg}^\eta = \left[\ln \frac{\hat{s} - M_{\eta_c}^2}{\mu_F^2} (2r^2 - 2r + 1) - 2(\ln(r) + 1)(r - 1)r \right] / r. \quad (\text{A.13})$$

After subtracting the logarithmically divergent parts of the NLO cross sections (attributed to the PDF) we have to average the remaining cross sections over the incoming subenergy \hat{s} , that is to integrate over r with the weight driven by the parton flux $F(\hat{s})$. Assuming the power behaviour $xg(x) \propto x^{-\Delta}$ of the low- x gluon distribution we obtain the flux $F \propto r^{-\Delta}$. Therefore, our goal is to choose such a scale $\mu_F^2 = \mu_0^2$ that nullifies the integral

$$\int_r^\infty \hat{\sigma}_{qg \rightarrow qM}^{NLO}(r, \mu_F) r^{-\Delta} \frac{dr}{r}. \quad (\text{A.14})$$

The resulting scales μ_0^2 depending on the subprocess and on the power Δ are presented in Table 2.

References

- [1] D. Diakonov, “QCD scattering: From DGLAP to BFKL,” CERN Cour. **50N6** (2010) 24.
- [2] H. -L. Lai, M. Guzzi, J. Huston, Z. Li, P. M. Nadolsky, J. Pumplin and C. -P. Yuan, “New parton distributions for collider physics,” Phys. Rev. D **82** (2010) 074024 [arXiv:1007.2241 [hep-ph]].
- [3] R. D. Ball, V. Bertone, F. Cerutti, L. Del Debbio, S. Forte, A. Guffanti, J. I. Latorre and J. Rojo *et al.*, “Impact of Heavy Quark Masses on Parton Distributions and LHC Phenomenology,” Nucl. Phys. B **849** (2011) 296 [arXiv:1101.1300 [hep-ph]].
- [4] R. D. Ball *et al.* [NNPDF Collaboration], “Unbiased global determination of parton distributions and their uncertainties at NNLO and at LO,” Nucl. Phys. B **855** (2012) 153 [arXiv:1107.2652 [hep-ph]].
- [5] A. D. Martin, W. J. Stirling, R. S. Thorne and G. Watt, “Parton distributions for the LHC,” Eur. Phys. J. C **63** (2009) 189 [arXiv:0901.0002 [hep-ph]];
- [6] V.B. Berestetskii, E.M. Lifshits and L.P. Pitaevskii, *Quantum Electrodynamics*, Reed Publishing (2002), p. 29.
- [7] Z. Conesa del Valle *et al.*, “Quarkonium production in high energy proton-proton and proton-nucleus collisions,” Nucl. Phys. Proc. Suppl. **214** (2011) 3 [arXiv:1105.4545 [hep-ph]].
- [8] Y. L. Dokshitzer, D. Diakonov and S. I. Troian, “Hard Processes in Quantum Chromodynamics,” Phys. Rept. **58** (1980) 269, Section 4.4.
- [9] E. G. de Oliveira, A. D. Martin and M. G. Ryskin, “Drell-Yan as a probe of small x partons at the LHC,” Eur. Phys. J. C **72** (2012) 2069 [arXiv:1205.6108 [hep-ph]].
- [10] J.H. Kuhn, J. Kaplan and E. G. O. Safiani, “Electromagnetic Annihilation of e^+e^- Into Quarkonium States with Even Charge Conjugation,” Nucl. Phys. B **157** (1979) 125.
- [11] R. Barbieri, R. Gatta and E. Remiddi, “Singular Binding Dependence in the Hadronic Widths of 1^{++} and 1^{+-} Heavy Quark anti-Quark Bound States,” Phys. Lett. B **61** (1976) 465.
- [12] R. Baier and R. Ruckl, “Hadronic Collisions: A Quarkonium Factory,” Z. Phys. C **119** (1983) 251.
- [13] J. P. Lansberg and T. N. Pham, “Effective Lagrangian for Two-photon and Two-gluon Decays of P-wave Heavy Quarkonium $\chi(c0, 2)$ and $\chi(b0, 2)$ states,” Phys. Rev. D **79** (2009) 094016 [arXiv:0903.1562 [hep-ph]].
- [14] J. Beringer *et al.* [Particle Data Group Collaboration], “Review of particle physics,” Phys. Rev. D **86** (2012) 010001.
- [15] M. A. Kimber, A. D. Martin and M. G. Ryskin, “Unintegrated parton distributions,” Phys. Rev. D **63** (2001) 114027 [hep-ph/0101348].
- [16] A. D. Martin, M. G. Ryskin and G. Watt, “NLO prescription for unintegrated parton distributions,” Eur. Phys. J. C **66** (2010) 163 [arXiv:0909.5529 [hep-ph]].
- [17] R. Gastmans, W. Troost and T. T. Wu, “Cross-Sections for Gluon + Gluon \rightarrow Heavy Quarkonium + Gluon,” Phys. Lett. B **184** (1987) 257.
- [18] R. Gastmans, W. Troost and T. T. Wu, “Production of Heavy Quarkonia from Gluons,” Nucl. Phys. B **291** (1987) 731.

- [19] R. Aaij *et al.* [LHCb Collaboration], “Measurement of the cross-section ratio $\sigma(\chi_{c2})/\sigma(\chi_{c1})$ for prompt χ_c production at $\sqrt{s} = 7$ TeV,” *Phys. Lett. B* **714** (2012) 215 [arXiv:1202.1080 [hep-ex]].
- [20] S. J. Brodsky, F. Fleuret, C. Hadjidakis and J. P. Lansberg, “Physics Opportunities of a Fixed-Target Experiment using the LHC Beams,” *Phys. Rep.* (2012), 10.1016 [arXiv:1202.6585 [hep-ph]].
- [21] J. P. Lansberg, S. J. Brodsky, F. Fleuret and C. Hadjidakis, “Quarkonium Physics at a Fixed-Target Experiment using the LHC Beams,” *Few Body Syst.* **53** (2012) 11 [arXiv:1204.5793 [hep-ph]].